Theory of light transmission through subwavelength periodic hole arrays

E. Popov, M. Nevière, Stefan Enoch, R. Reinish

Theory of light transmission through subwavelength periodic hole arrays

E. Popov,[1]* M. Nevière,[2] S. Enoch,[2] and R. Reinisch[3]
[1]*Institute of Solid State Physics, 72 Tzarigradsko Chaussee Boulevard, 1784 Sofia, Bulgaria*
[2]*Laboratoire d'Optique Electromagnétique, UPRES A CNRS no 6079, Faculté des Sciences de Saint-Jérôme, Case 262, 13397 Marseille Cedex 20, France*
[3]*Laboratoire d'Electromagnétisme, Microondes et Optoélectronique, UMR CNRS no 5530, 23, Avenue des Martyrs, Boîte Postale 257, 38016 Grenoble Cedex, France*
(Received 2 August 2000)

The existing theories which aim to explain the extraordinary optical transmission of a metallic film pierced by a two-dimensional subwavelength hole array [T.W. Ebbesen, H.J. Lezec, H.F. Ghaemi, T. Thio, and P.A. Wolff, Natural (London) **391**, 667 (1998)] all have in common the following feature: instead of studying the two-dimensional crossed grating resulting from the hole array, they consider a one-dimensional grating with infinite slits. We show that such a simplification introduces an efficient channel for light transmission in lamellar gratings, *which does not exist for hole arrays*. Therefore in order to explain the relatively high transmission observed by Ebbesen *et al.*, it is necessary to take into account the existence of the holes in the array. In this paper we develop a two-dimensional analysis of the experiment performed by Ebbesen *et al.* No simplification is introduced. This allows us to obtain theoretically the long-wavelength peak reported by Ebbesen *et al. with the same grating thickness as the one used by these authors*. We also review and study in detail the various contributions devoted to this very surprising effect.

I. INTRODUCTION

The famous paper by Ebbesen *et al.*[1] which showed that subwavelength hole arrays inside a silver film can present a light transmission much higher than the hole surface-to-total surface ratio has stimulated a wide interest in the scientific community. Although the photon tunneling effect is well known since many years and is widely used in near-field microscopy,[2–6] the discovery of the above-mentioned extraordinary transmission surprised their authors, as well as other physicists. Indeed a rapid estimation of the attenuation length of evanescent waves involved in the photon-tunneling process shows that the origin of the extraordinary transmission is of a different nature. Several authors thought to relate this surprising effect to the excitation of surface plasmons.[7–10] This seems quite natural since it has been established[11] that surface plasmons are responsible for a type of grating anomalies. However, other kinds of electromagnetic resonances may play similar roles, for example eigenmodes inside cavities or waveguides.[9,12] Thus other authors[13,14] also attributed the effect to the excitation of cavity resonances, i.e., of localized surface shape resonances, while the classical surface plasmons are delocalized resonances. All these authors simulate the observed transmission spectrum via electromagnetic computations concerning one-dimensional gratings. However, Ebbesen *et al.*[1] dealt with crossed gratings[15–18] constituted of hole arrays. Studying such a situation rises a challenge to all scientists familiar with the electromagnetic theory of gratings.[19] It is worth noting that some waveguide resonances of the one-dimensional model do not exist considering hole arrays. Indeed, as is well known, TEM (in the sense of classical waveguide theory[20]) waveguide resonances cannot exist in waveguides whose cross section is a simply connected domain.[20] Consequently, TEM resonances exist in metallic gratings with infinite slits but do not exist in Ebbesen's two-dimensional gratings.[1] As compared to TE and TM modes, TEM modes have a zero cutoff frequency. Consequently these TEM modes constitute an efficient channel for light transmission in lamellar gratings.[9,12–14] Unfortunately such a channel cannot be invoked to explain the highest wavelength resonance peak.[1] It is also necessary to notice that with a grating thickness of 0.2 μm (the thickness of the experiment reported in Ref. 1), the waveguide resonance discussed in Ref. 9 does not exist. This discussion clearly points to the necessity of using a rigorous electromagnetic theory of crossed gratings with finite conductivity.[15–18,21] It is the aim of this paper to present such an analysis. No simplification is introduced in our approach. This allows us to obtain the long-wavelength peak with the same grating thickness (0.2 μm) as in Ref. 1.

For the sake of completeness, we first review, in Secs. II and III, the various resonances (cavity resonances, surface plasmon resonances) that produce anomalies in reflection and transmission spectrum of gratings. The study of field maps allows finding the origin of the light transmission peaks through lamellar gratings. This is achieved with computer codes based on the rigorous electromagnetic theories of gratings with finite conductivity.[22–24] Section IV is devoted to the bidimensional study of Ebbesen *et al.* experiment.[1]

II. CAVITY RESONANCES

When considering this type of electromagnetic resonances, a difficulty comes from the terminology. Indeed considering one-dimensional gratings the TE, TM decomposition is performed with respect to the z component (Fig. 1) of the electric or magnetic fields, respectively.[19] This is the decomposition of the opticians. Another decomposition, which is always valid, i.e., even when the system is not z invariant, is that used in waveguide theory.[20] In this case, the TE and

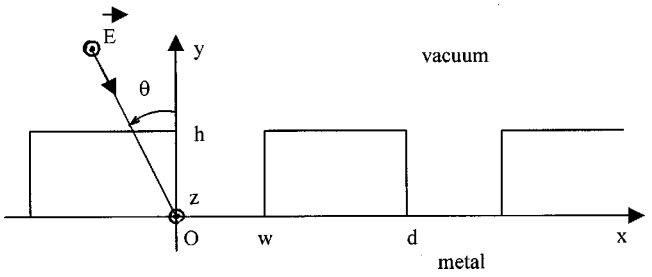

FIG. 1. Schematic representation of a lamellar grating.

TM polarizations refer to solutions that have no electric or magnetic field component along the direction of propagation, respectively. Another class of solutions, which refer to TEM polarization, is known to have no cutoff frequency, since its determination requires resolving the Laplace equation instead of the Helmholtz one. They are also known to require a waveguide with a nonsimply connected cross section in order to exist. Hence the very important consequence: there is no TEM wave inside a perfectly conducting hose, whatever its simply connected cross section may be. This conclusion fails if the section is unbounded. It is then possible to propagate a TEM wave between two infinite parallel perfectly conducting planes, and the wavevector of the TEM mode is the same as in the unbounded space. In order to distinguish the three classes of polarizations used in waveguide theory from the TE, TM cases of the opticians, we use the subscript ''wg'' namely TE_{wg}, TM_{wg}, TEM_{wg}.

Cavity resonances have been involved in the explanation of lamellar diffraction gratings anomalies. In 1979, Andrewartha *et al.*[25,26] studied perfectly conducting lamellar gratings in detail, and discovered that modes exist inside the grooves, their number depending on the groove width and wavelength. When these modes are excited, they cause a strong redistribution of energy into the different diffracted orders, the transfer from mode resonances towards far-field resonance depending on wavelength and groove depth. These cavity resonances, which explained anomalies in the reflected orders of lamellar gratings, exist for both TE and TM polarization and may play a similar role for the transmitted field of a rectangular rod grating.

The use of the perfectly conducting model is not sufficient for the present study. As previously pointed out,[12] the perfect conductivity prevents the coupling of the field in the neighboring grooves directly through the lamella walls. On the other hand, the finite conductivity of the lamellae causes the tangential component of the electric field on the surface to differ from zero. This leads to absorption losses, which may result into a phenomenon of total absorption.[27] Thus the finite conductivity may play a non-negligible role and has to be taken into account in a study which aims to bring quantitative results.

The main features of cavity resonances will be pointed out on the lamellar grating illustrated in Fig. 1, and previously studied in Ref. 12. The grating has period d, groove depth h, and groove width w. It is lighted by a TE polarized incident plane wave with wavelength λ under incidence θ. The superstrate is vacuum, the substrate and the bumps are filled with a metal whose refractive index is $0.4+i4.4$. In this section, we choose $\lambda=1\ \mu$m, $\theta=0°$, $d=2.99\ \mu$m, $h=1\ \mu$m. As pointed out in Ref. 12, when the groove width w is varied, several anomalies (dips) occur in both the zeroth-order efficiency and the total-reflected energy curve, each of them corresponding to the excitation of a cavity mode. Figure 2 shows the total field intensity map of the fundamental mode, which is excited when $w/d=0.16$, for $x\in[0,w]$ and $y\in[0,h]$. One can see that $|E_z|^2$ is null at the bottom of the grooves ($y=0$) and small on the vertical walls ($x=0$ and $x=w$, with $y\in[0,h]$). The maximum of $|E_z|^2$ is located close to the center of the cavity. However, since we deal with an open resonator, $|E_z|^2$ is not null at the top of the groove, which allows a coupling with the diffracted field. When w is increased, higher modes appear, and the chosen normal incidence precludes the existence of odd modes. Figure 3 shows the field map of a more complex mode which is resonantly excited when $w/d=0.5016$. Four maximums are observed instead of one, but the same comments apply as for the fundamental mode. The existence of downgoing and upgoing modes in the grooves (i.e., along y) leads to cavity resonances and explains the y dependence of the electric field. In particular, we can see in both Figs. 2 and 3 that at the top of the grooves ($y=h$), the maximum value $|E_z|^2$ is about 5, while the incident wave amplitude is assumed to be unity. It means that such resonances do not produce a noticeable field enhancement near the grating surface, nor in the far field, the maximum value of E_z being limited to about twice the one of the incident wave. Although the width of the lamellas in Fig. 3 are much thinner than that in Fig. 2, the field on the vertical walls is still small, showing a negligible coupling between the modes in the neighboring grooves, as it occurs in the perfectly conducting model. As a result, the cavity resonances of a lamellar grating do not significantly depend on

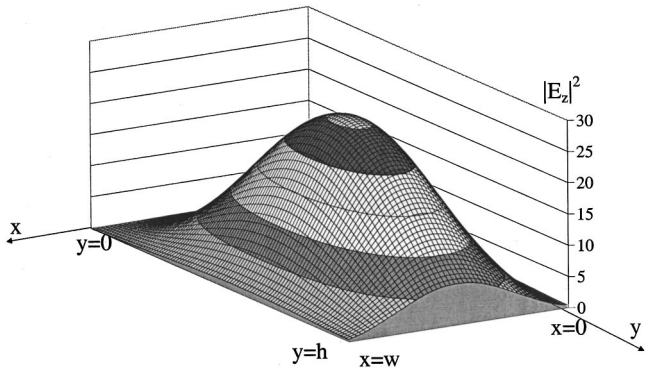

FIG. 2. Field map of the fundamental cavity mode.

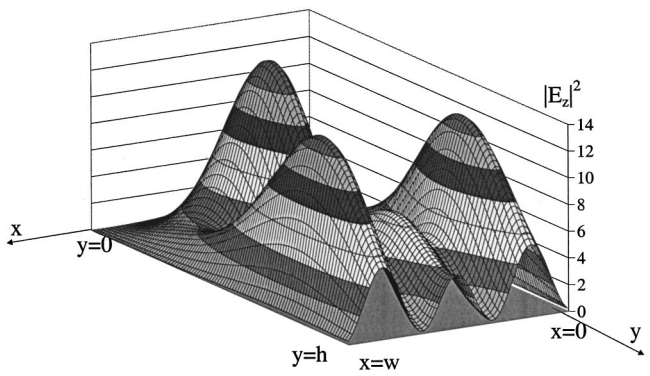

FIG. 3. Field map of a higher order cavity mode.

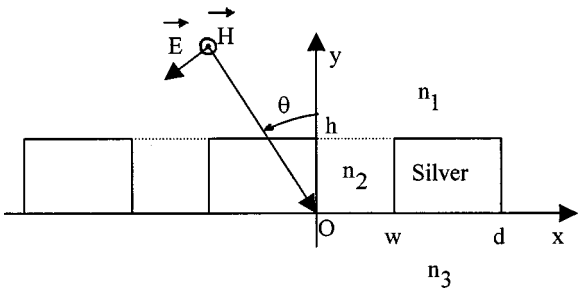

FIG. 4. Rectangular rod grating and notations.

the bump width, and thus, of the period, while they strongly depend on the groove width and groove depth.

These comments done for TE waves also apply for TM modes. We have to remember, however, that the TE and TM cutoff frequencies are different so that, for a groove width small enough, one of the two kinds of modes may propagate. A third kind of modes, namely the TEM_{wg} one, may also occur. We are now in position to understand and to discuss the work presented in Refs. 9 and 14.

The authors of Refs. 9 and 14 explain the extraordinary optical transmission[1] of a two-dimensional subwavelength hole array by analyzing a one-dimensional model, i.e., a lamellar metallic grating. Their device is shown in Fig. 4, where n_1, n_2, and n_3 are the refractive indices of the various regions. The metal is silver, whose refractive index at the chosen 1.433 μm wavelength is equal to $0.134+i10.462$. A TM polarized incident field is considered, as illustrated in Fig. 4 and, in Refs. 9 and 14, it is assumed that the mode profile inside the grooves is the same as that of the perfectly conducting case. In order to discuss their works and conclusions, we first analyze the case where the grating is lighted in TE polarization. We chose the grating parameters described in Fig. 2 of Ref. 14, i.e., $d=0.9\,\mu$m, $h=1.8\,\mu$m, $\theta=0°$; $n_2=n_1=1$; $n_3=1.5$, and we chose $w=0.04\,\mu$m, near which appears the cavity anomaly (see Fig. 2 of Ref. 14). Figure 5(a) shows the field intensity map inside a groove, i.e., $x\in[0,w]$, $y\in[0,h]$. One can see that the field intensity, which is already small at the top of the groove, exponentially decays inside it, so that the field is almost null everywhere. The exponential decrease of $|E_z|^2$ as a function of y is confirmed by Fig. 5(b). Thus no field exists at the bottom, and the transmittance is zero. This confirms our previous experience of the filtering properties of such gratings[28] and shows that the 0.04 μm value of w is below the TE mode cutoff. As previously pointed out in Refs. 28 and 14, the TM polarization case does not suffer from such a limit, so that such a device has polarizing properties. This is a surprising result for people acquainted with waveguide theory. In waveguide theory, both TE_{wg} and TM_{wg} modes have cutoff phenomena. Thus nobody would expect that a vertical metallic rectangular waveguide made by limiting in the z direction the two vertical walls of a groove will support propagating TM_{wg} modes when its width tends to zero; moreover the fundamental TM_{wg} mode would be expected to disappear before the fundamental TE_{wg} one, which is indeed the fundamental mode for the $TE_{wg}+TM_{wg}$ family. This apparent contradiction is blown away when one realizes that the TM field studied in Refs. 9, 14, and 28 has, inside the grooves, an electric vector perpendicular to the vertical walls of the groove and

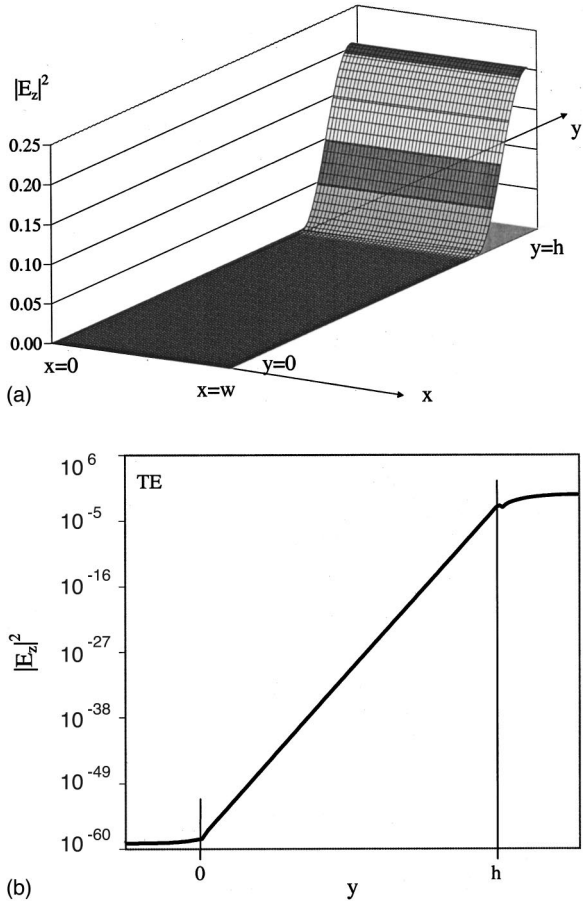

FIG. 5. (a) Field intensity map inside a groove in TE polarization; (b) y dependence of the field intensity obtained at $x=w/2$ shown on a logarithmic scale.

that this field is a TEM_{wg} one, with the terminology of waveguide theory, for which, as already stated, no cutoff frequency exists.

Indeed, when we repeat the same calculations as those which led to Fig. 5, but for TM polarization, we find the results shown in Fig. 6. In order to obtain orders of magnitudes similar for both electric and magnetic field, $|Z_0H_z|^2$ is plotted instead $|H_z|^2$, where Z_0 is vacuum impedance. One can see that $|H_z|^2$ is almost constant with respect to x, which legitimates the assumption done in Refs. 9 and 14 which consisted in choosing the mode profile equal to that of the perfectly conducting case, equal to $\mathrm{rect}(x/w)$. Concerning

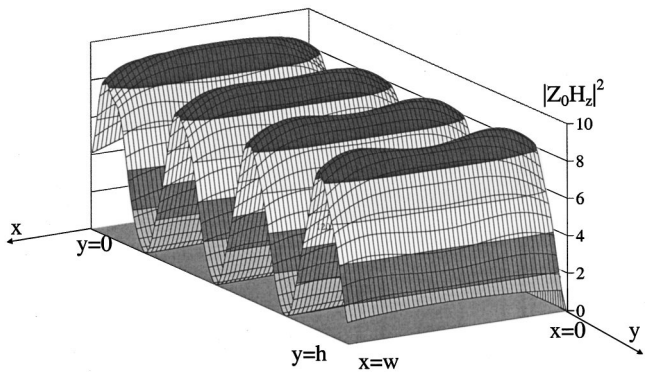

FIG. 6. Magnetic field intensity map in TM polarization.

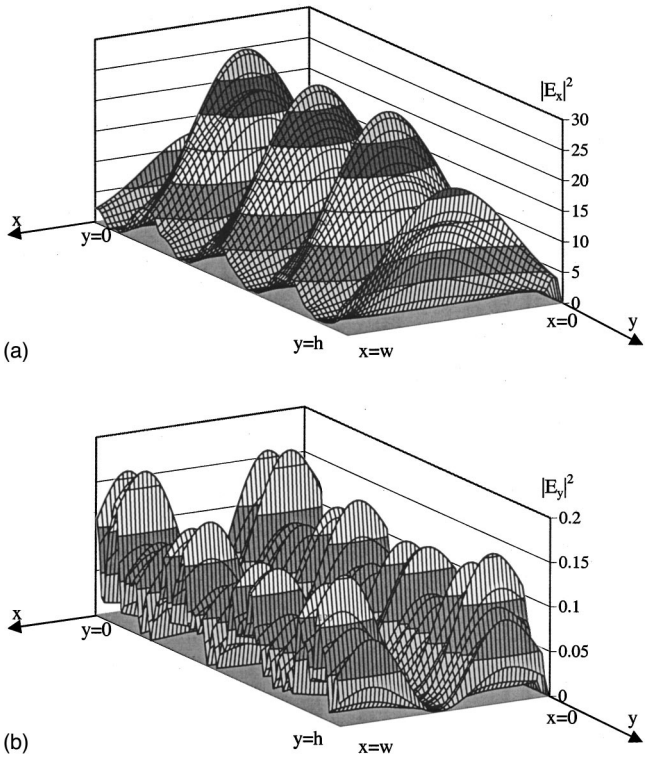

FIG. 7. Electric field map intensity in TM polarization (a) $|E_x|^2$ map; (b) $|E_y|^2$ map.

the y variation, sinusoidal oscillations are observed. Such oscillatory behavior has been predicted[28] by a simplified version of the modal theory of lamellar gratings in which only one mode is kept to represent the field in the grooves. The field is, then, the sum of a downgoing and an upgoing wave, and can be calculate by a Bremmer series[29] identical to the one used in the Fabry-Perot theory.[30] Thus, as expected from the Fabry-Perot behavior, the number of maximums depends on groove depth h, as we verified by nonreported calculations. As shown in Fig. 7(a), the minimums of $|H_z|^2$ correspond to maximums $|E_x|^2$ and vice versa; Fig. 7(b) shows that $|E_y|^2$ presents a more complicated x variation, while its y variation presents the same minima as for $|H_z|^2$.

The combination of the $\vec{H}$ and $\vec{E}$ field maps result in the total energy map illustrated in Fig. 8. From the nonzero value of the energy density at the bottom of the groove, one expects a significant transmittance which will depend on w and h, linked with a dip in reflectivity. For a fixed groove

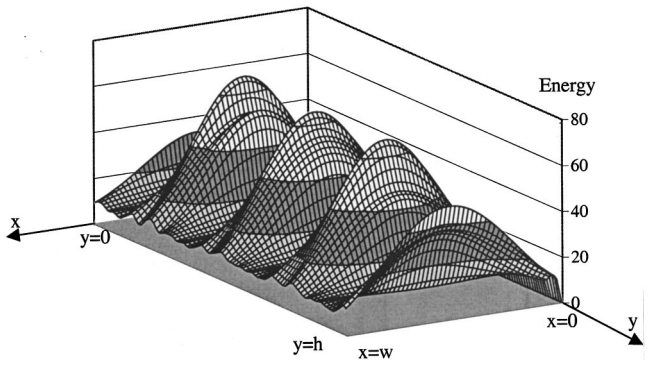

FIG. 8. Total energy map in TM polarization.

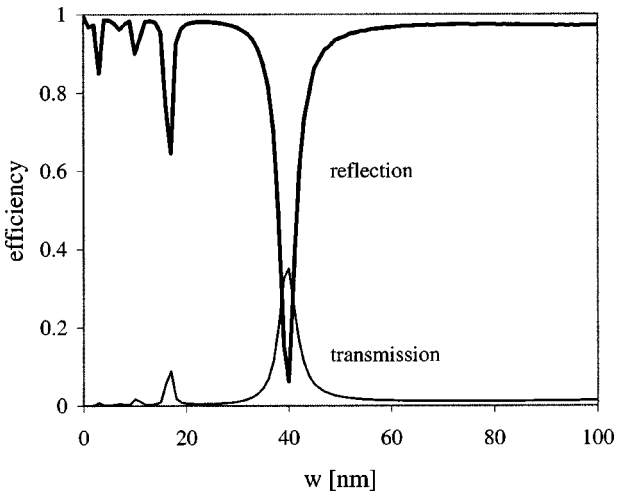

FIG. 9. Reflectivity and transmittivity curves as function of the groove width w.

depth equal to 1.9 μm, and other parameters as those used in Fig. 5, Fig. 9 shows the reflectivity and transmittance curves as functions of w. Several dips and peaks occur. Let us analyze the two strongest, which occur for $w=17$ nm and $w=39.7$ nm.

In Fig. 10, we choose a fixed abscissa corresponding to the center of a slit, $(x=w/2)$, and analyze the $|H_z|^2$ curve as a function of ordinate y inside the modulated area. Such a curve is drawn for the value of w corresponding to the maximum of transmittance ($w=39.7$ nm) and for a value far from the peak, at which the transmittance is negligible ($w=50$ nm). The vertical lines show the limits of the modulated area. Noticing that the ordinate scale is logarithmic, it is clear that when the maximum transmittance occurs, $|H_z|^2$ is much higher, and a finite number of maxima are included in the modulated region. Similar conclusions are derived from the curves in Fig. 11. They confirm what is known in Fabry-Perot's resonators.[30]

To conclude this paragraph, the $\mathrm{TEM_{wg}}$ guided mode explains the important optical transmission of a metallic lamellar grating with subwavelength slits reported in Refs. 9 and 14. However, since the $\mathrm{TEM_{wg}}$ mode does not exist in me-

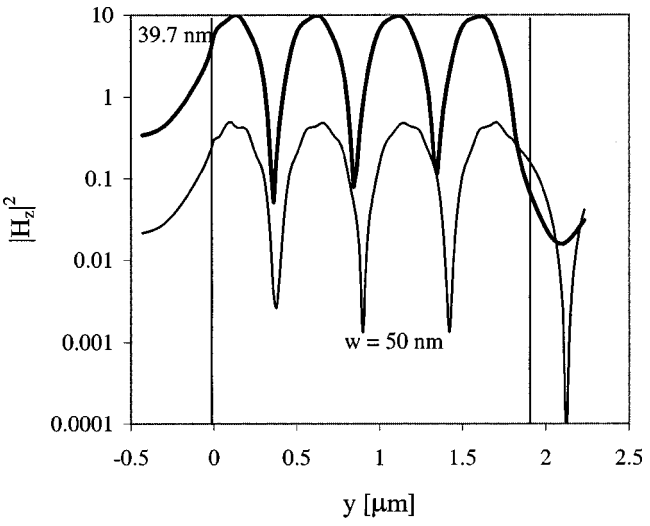

FIG. 10. Magnetic field intensity oscillations inside a groove.

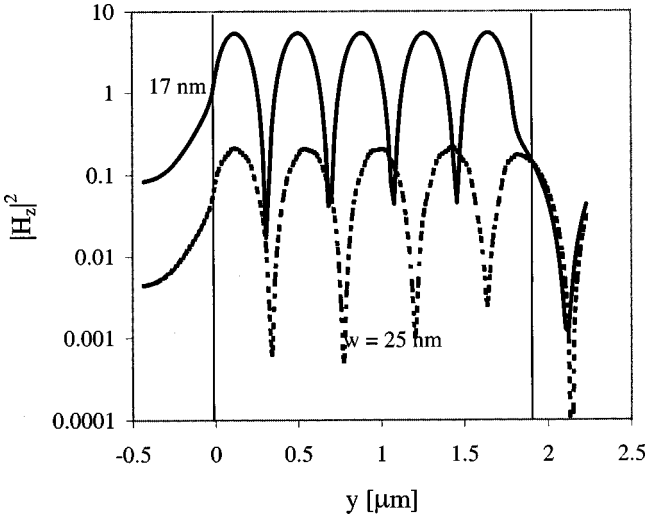

FIG. 11. Same as in Fig. 10, but for the second main transmittance peak.

tallic holes, the one-dimensional model cannot be used to explain the phenomenon reported in Ref. 1 which is concerned by a hole array. This remark concerns all works which have used the one-dimensional model to explain the discovery presented in Ref. 1. But before considering the hole array system, let us discuss the surface plasmon resonances which can also be excited in the geometry of Figs. 1 or 4.

III. SURFACE PLASMON RESONANCES

In order to illustrate the main features of the surface-plasmon resonance, we choose the device previously studied in the Fig. 3(a) of Ref. 9. It consists of a rectangular rod silver grating; with the notations in Fig. 4, $n_1=n_2=n_3=1$; $d=3.5\,\mu$m, $h=0.6\,\mu$m, $\lambda=3.6\,\mu$m, $\theta=0°$; the refractive index of silver is $0.1+i10$. With the chosen parameters, a delocalized surface plasmon is excited, and, as pointed out in Ref. 9, a strong field is expected near the entire grating surface. We present the computed field maps obtained in such a situation.

Figure 12 shows the magnetic field intensity map inside and near the modulated area. Above the silver rectangular

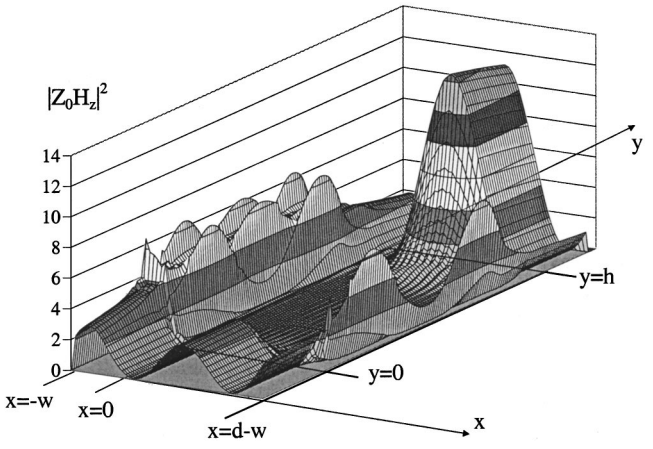

FIG. 12. Magnetic field intensity map of a surface plasmon resonance.

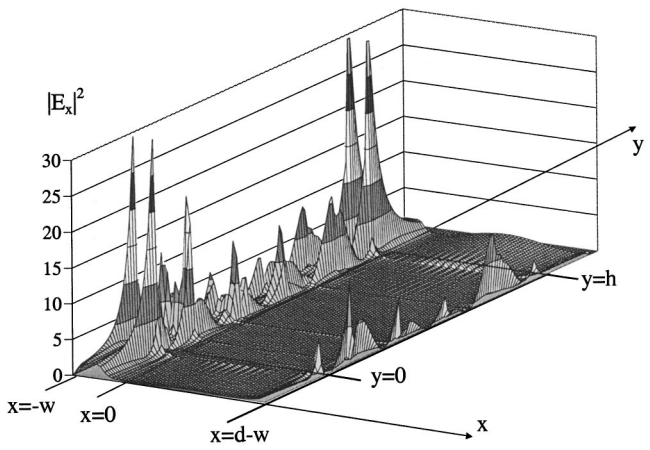

FIG. 13. $|E_x|^2$ map of the device in Fig. 12.

rod, $(0<x<d-w)$ $|H_z|^2$ has a strong maximum, which is expected since, in the perfectly conducting limit, the jump of H_z leads to a surface current. Of course, for a real metal, $|H_z|$ exponentially decreases inside the metallic rod. However, one can see that $|H_z|^2$ has significant values in the slit, $(-w<x<0)$ which allows a coupling between the bottom and top surface of the rod grating. As a result, a non-null H_z is found below the grating.

Figure 13 shows the $|E_x|^2$ map of the same device. In the finite conductivity limit, E_x is expected to vanish on the metal surfaces $y=h,0$; as a result, the values of $|E_x|^2$ are indeed small on the rod surface. Edge phenomena are seen at the corners of the rods, and a coupling is still observed between upper and lower interfaces.

In Fig. 14, $|E_y|^2$ is plotted, and presents, as expected, high values near the metal surfaces $y=h,0$. The excitation of surface plasmons propagating in the x direction is made on both upper and lower interfaces, as evident in the figure.

Figure 15, which presents the total energy map, confirms the previous conclusions drawn from Figs. 12–14, i.e., that the delocalized surface plasmon resonance produces strong near-field outside the modulated area $(0<y<h)$, while both fields and energy are weak inside the slits. In order to stress the big difference with the cavity resonances studied in Sec. II, Fig. 16 show the same maps as in Figs. 12–15, but for $h=3\,\mu$m and $\lambda=7.5\,\mu$m for which a cavity resonance is excited. It is clearly shown that, this time, both field and energy are strong inside the slits, while they remain small

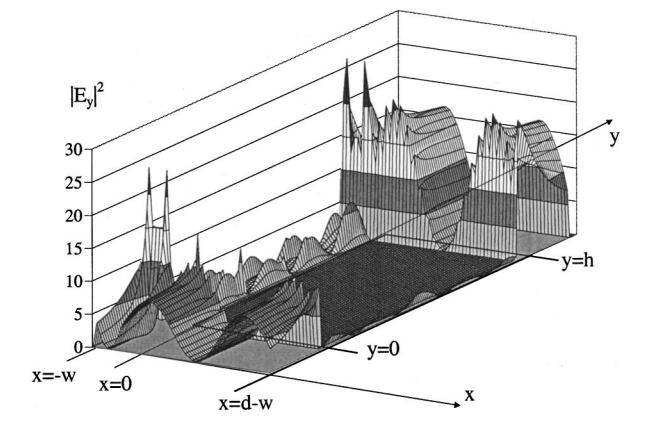

FIG. 14. $|E_y|^2$ map of the device in Fig. 12.

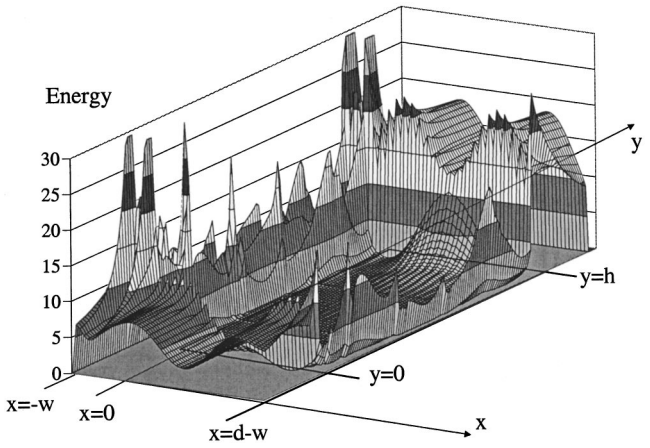

FIG. 15. Total energy map of the device in Fig. 12.

outside the modulated area. This effect has previously been used to explain enhanced nonlinear optical effects, e.g., surface-enhanced Raman scattering of organic molecules absorbed on a rough surface,[31] although delocalized surface plasmons are also involved in the explanation of other enhanced nonlinear effects.[32] Our field maps confirm and state precisely the arguments developed in Ref. 9.

Now that we have reviewed the electromagnetic resonances involved in one-dimensional systems, let us consider the case of two-dimensional gratings.

IV. ELECTROMAGNETIC STUDY OF A 2D-SUBWAVELENGTH SQUARE HOLE ARRAY

In order to analyze the two-dimensional hole array, we choose the Fourier modal method extended to crossed gratings.[21] This method is well suited for crossed surface relief gratings consisting of vertical cylindrical holes inside a metallic or a dielectric plate in the sense that the Fourier components of the permittivity function are independent of ordinate, and that the problem reduces to an eigenvalue one, which has only to be resolved once. An additional small simplification is obtained by considering square hole cross-sections instead of circular ones (which leads to a simpler expression for the permittivity Fourier components, and allows working in an orthogonal coordinate set, which greatly simplifies the propagation equations). In order to deal with high reflecting materials, the *S*-matrix propagation algorithm[33,34] is included. The convergence of the double Fourier series of the field is improved by using the correct rules for Fourier factoring products that contain discontinuous functions.[35–37] Computations have shown that it is possible to obtain converging numerical results for the transmittivity of various hole arrays inside a silver plate. Also our method allows determining the propagation constant along the hole axis of symmetry of all propagating (and evanescent) modes, a problem which reduces to the search of eigenvalues of a particular matrix.

Indeed, if (x,z) is the grating plane and y the coordinate

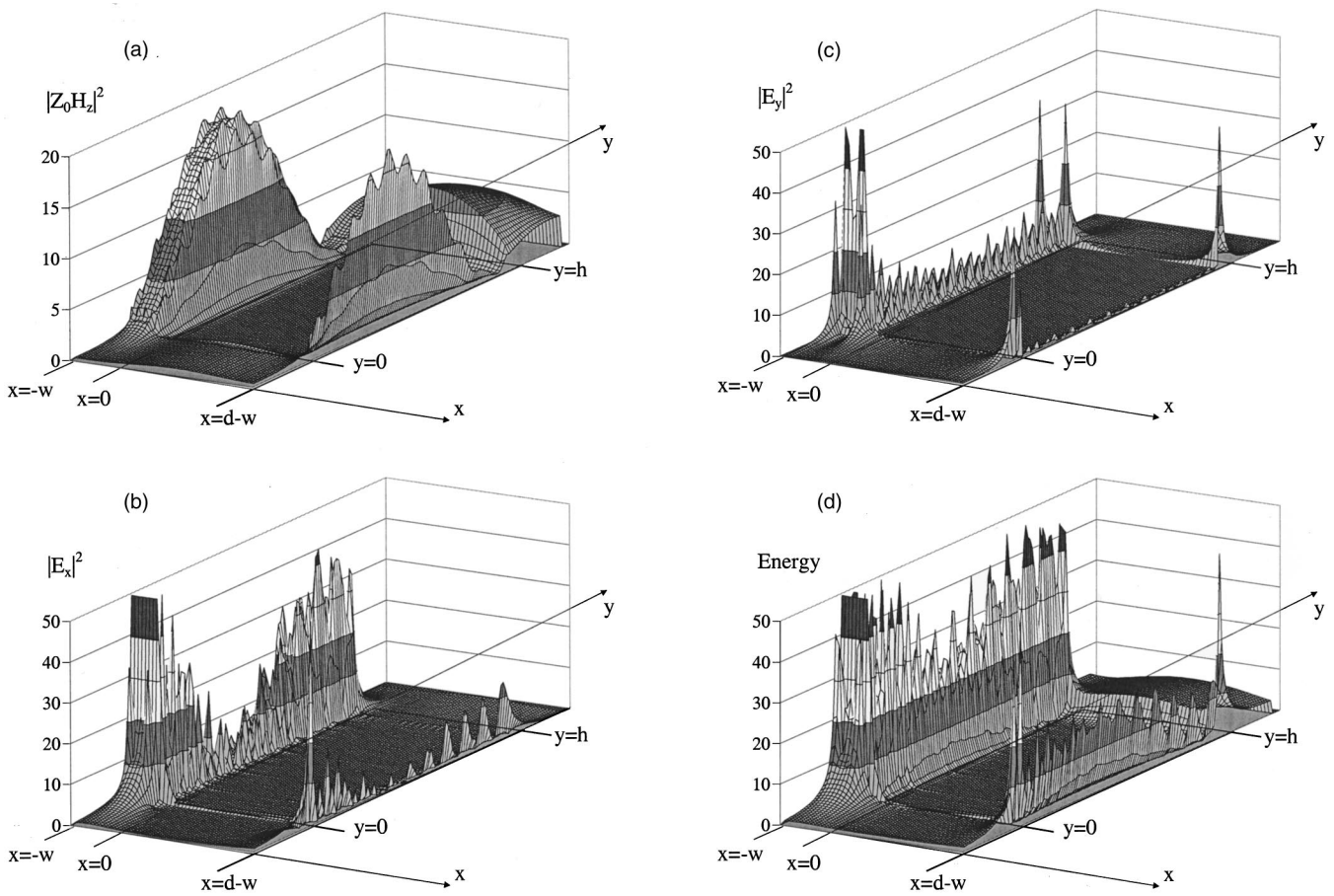

FIG. 16. Field and energy maps associated to a cavity resonance of a device similar to the one studied in Figs. 12–15. (a): $|H_z|^2$ map; (b): $|E_x|^2$ map; (c): $|E_y|^2$ map; (d): total energy map.

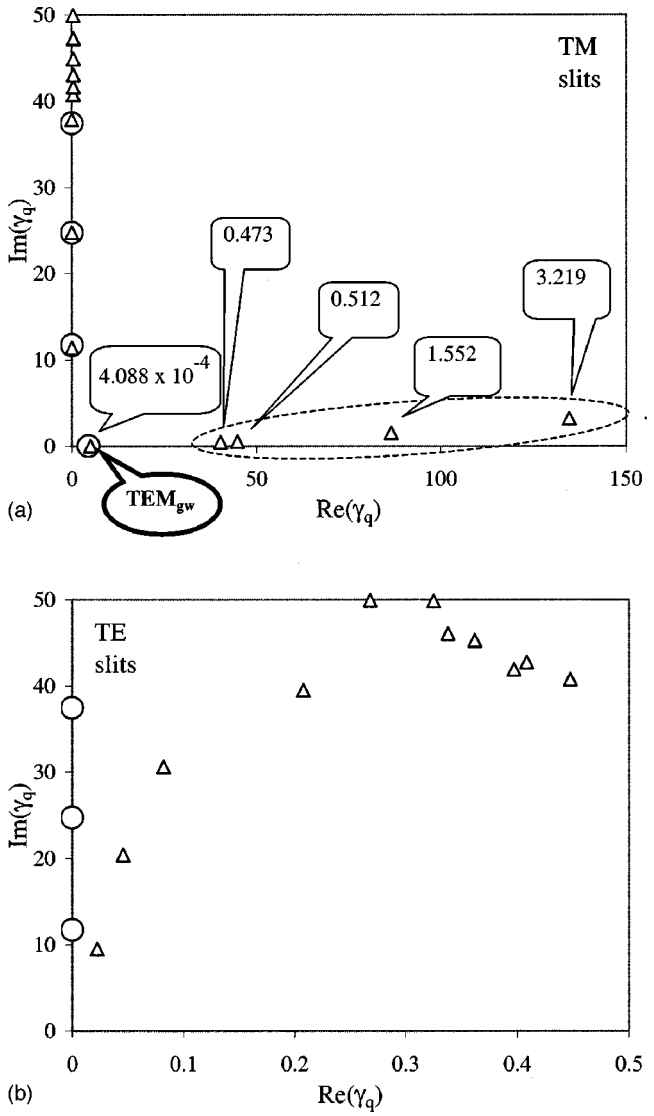

FIG. 17. Eigenvalues (vertical mode propagation constants) of a silver grating with infinite slits in the complex γ_q plane for TM polarization (a) and for TE polarization (b). Circles: infinite conductivity, triangles: finite conductivity. The numerical values shown in the bubbles correspond to Im(γ_q). Notice, for TM polarization (i) the existence of the $\mathrm{TEM_{wg}}$ solution which has the lowest Im(γ_q) and (ii) within the dashed boundary, low values of Im(γ_q) which *only* exist in the case of *finite* conductivity.

along the grating normal, any field component inside the square holes writes:[33]

$$E_\sigma(x,y,z)=\sum_{m,n,q}\left[u_q\exp(i\gamma_q y)+v_q\exp(-i\gamma_q y)\right]\times\exp[i(\alpha_m x+\beta_n z)]E_{\sigma\mathrm{mnq}},$$

where $\sigma=x,z$ and u_q and v_q are the amplitudes of the upward and downward propagating or decaying modal fields. In the subwavelength region, *all* modes inside the holes are evanescent, so that the field intensity below the hole array is mainly governed[28] by the mode which has the lowest attenuation constant, i.e., by the mode for which Im(γ_q) is minimum. In what follows, we will simply call γ the corresponding propagation constant.

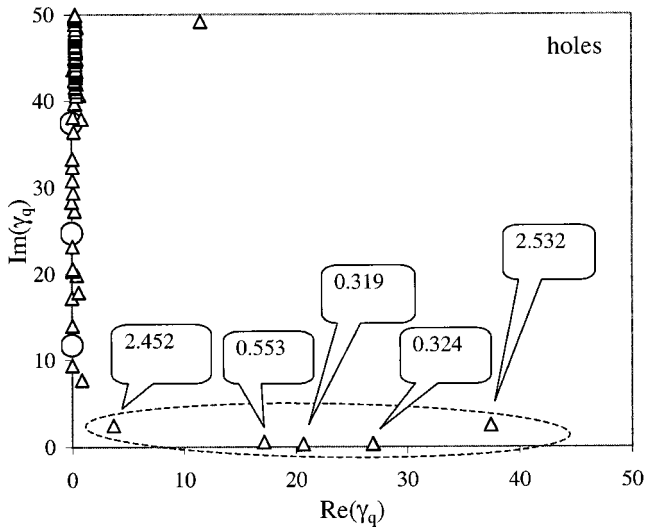

FIG. 18. Same as Figs. 17 but for a square hole array in a silver plate. Circles: infinite conductivity, triangles: finite conductivity. The numerical values in the bubbles correspond to Im(γ_q). Notice the lack of the $\mathrm{TEM_{wg}}$ solution. The triangles within the dashed boundary correspond to low values of Im(γ_q) which *only* exist in the case of *finite* conductivity.

For a better understanding of the origin of the light transmission peaks, it is appropriate to consider, for both the infinite and finite conductivity cases, the channels for light transmission not only for the hole array but also for the one-dimensional lamellar grating.

Figures 17 and 18 show the various γ_q in the complex plane for a lamellar grating with infinite slits [Figs. 17(a) and 17(b) for the TM and TE cases, respectively] and for a square hole array in a silver plate (Fig. 18). The x and z periods of the array are 0.9 μm, the square width 0.25 μm and the thickness of the plate 0.2 μm; it is lighted under normal incidence with a 1.37 μm wavelength at which refractive index of silver is $0.1+i8.94$.

Examination of Figs. 17 show three classes of solutions: (i) imaginary values of γ_q; (ii) in the TM case and for finite conductivity only, within the dashed boundary, complex values of γ_q with low imaginary part of γ_q and (iii) the $\mathrm{TEM_{wg}}$

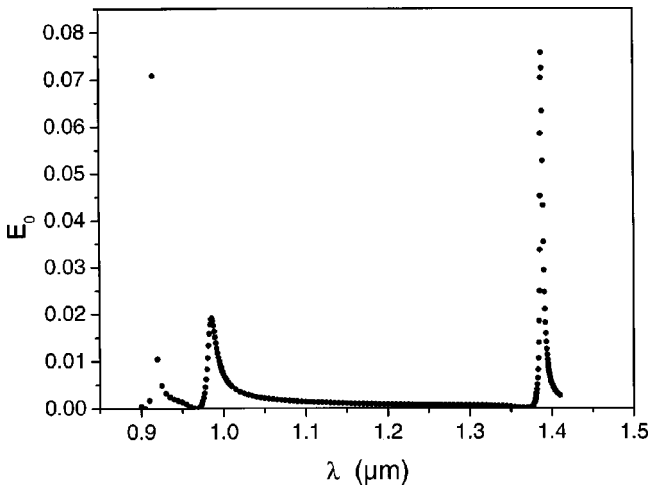

FIG. 19. Computed transmitted intensity of a square hole array in silver.

solution. The latter is not excited in the TE case and has a nearly zero imaginary part when the silver losses are taken into account. Thus, as already explained, the TEM_{wg} solution constitutes an efficient channel of transmission for light when lamellar gratings are involved.

Let us now consider Fig. 18. First of all, the TEM_{wg} channel presented in Fig. 17(a) no longer exists. As in Fig. 17(a), for finite conductivity, complex values of γ_q are obtained (they are located within the dashed boundary) with the imaginary part much lower than for infinite conductivity. Indeed, inside a perfectly conducting waveguide, the fundamental cutoff wavelength is twice the square width, i.e., 0.5 μm from which we deduce $\gamma^2=4\pi^2/\lambda^2-\pi^2/a^2=-129.0973\,\mu\mathrm{m}^{-2}$. The result is that $\mathrm{Im}(\gamma)=11.362\,\mu\mathrm{m}^{-1}$, so that a wave of the form $v_q\exp(-i\gamma_q y)$ is attenuated from top to bottom of the hole by a factor $\exp[-\mathrm{Im}(\gamma)h]\approx 0.00534$. For finite conductivity, one can find γ with much lower imaginary part, e.g., $\mathrm{Im}(\gamma)=2.4\,\mu\mathrm{m}^{-1}$, i.e., $\exp[-\mathrm{Im}(\gamma)h]\approx 0.6$. It means that the transmitted field energy is 10^4 times larger when the finite conductivity of silver is taken into account. Thus it is seen that hole array with finite conductivity supports an efficient channel for the transmission of light despite the fact that there is no TEM_{wg} solution. Such a result is all the more surprising that in the considered spectral region the reflectivity of silver is close to 99%. This channel yields the peak observed in Fig. 1 of Ref. 1 close to 1.37 μm wavelength, as shown in Fig. 19. The excitation of surface plasmons on the upper interface (causing the peak around 0.9 μm in Fig. 1 of Ref. 1) is easily made using the $\pm$1st diffracted order ($\lambda/d\approx 1$). The channel is responsible for the excitation of surface plasmons on the lower interface with constant of propagation of the order of 1.5 (the substrate refractive index is equal to 1.5) again through the $\pm$1st diffracted order in the substrate. This happens for $\lambda/d\approx 1.5$, i.e., $\lambda\approx 1.35$ and is the cause for the longer-wavelength peak in Fig. 1 of Ref. 1 (same as in Fig. 19). Our numerical investigations, not reported here, have shown that when varying the periodicity d, the peak position remains constant in the λ/d scale. Its position does not depend significantly on the hole dimensions, which would not be the case if cavity resonances were excited. Moreover, the layer thickness (0.2 μm) is too small to involve a cavity resonance. It is worth noting that the same kind of channel exists for lamellar gratings in TM polarization [within the dashed boundary in Fig. 17(a)]: the finite conductivity generates an additional set of eigenvalues with lower imaginary parts. However, for one-dimensional gratings their effect in transmission is masked by the existing TEM_{wg} mode, which does not propagate in the holes.

As it was done in Ref. 1, it is interesting to replace silver by germanium. Taking a refractive index equal to 3.5, we have computed the propagation constants of the same hole array. It was found that one of them is real, which leads to uniform contribution to the transmitted intensity, while the closest eigenvalue has an imaginary part three times higher than the one found with silver, which precludes any resonant contribution with the chosen thickness. Our results also allows predicting that the transmittivity of the array scales linearly with the surface area. Concerning the thickness dependence, it is governed by the $\exp[-\mathrm{Im}(\gamma)h]$ term, which, for thin thicknesses, can be approximated by a linear function. All our results account for what is observed in Ref. 1.

CONCLUSION

We have reviewed and studied in detail the various resonant processes which were previously invoked to explain the transmission of light through subwavelength hole arrays. For one-dimensional lamellar gratings, cavity and surface plasmon resonances account for several observed maxima; cavity resonances arise from the excitation of TEM_{wg} solutions. However, no TEM_{wg} solution is present in the case of hole arrays. For such systems we have demonstrated the existence of a channel for the transmission of light that cannot be predicted by one-dimensional models. This channel, which allows the resonant excitation of surface plasmons on the lower interface, is specific of two-dimensional hole arrays with finite conductivity and explains the extraordinary optical transmission of these devices.

*Temporary Address: Laboratoire d'Electromagnétisme, Microondes et Optoélectronique, UMR CNRS, no. 5530, 23, Avenue des Martyrs, Boîte Postale 257, 38016 Grenoble Cedex, France.

[1] T. W. Ebbesen, H. J. Lezec, H. F. Ghaemi, T. Thio, and P. A. Wolff, Nature (London) **391**, 667 (1998).
[2] E. Betzig, A. Harootunian, M. Isaacson, and E. Kratshmer, Biophys. J. **49**, 269 (1986).
[3] U. Düring, D. W. Pohl, and F. Roher, J. Appl. Phys. **59**, 3318 (1986).
[4] D. Courjon, K. Sarayeddine, and M. Spajer, Opt. Commun. **71**, 23 (1989).
[5] R. C. Reddick, R. J. Warmack, and T. L. Ferrell, Phys. Rev. B **39**, 767 (1989).
[6] F. de Fornel, J. P. Goudonnet, L. Salomon, and E. Lesniewska, Proc. SPIE **1139**, 77 (1989).
[7] U. Schröter and D. Heitmann, Phys. Rev. B **58**, 15 419 (1998).
[8] M. M. J. Treacy, Appl. Phys. Lett. **75**, 606 (1999).
[9] J. A. Porto, F. T. Garcia-Vidal, and J. B. Pendry, Phys. Rev. Lett. **83**, 2845 (1999).
[10] H. F. Ghaemi, T. Thio, D. E. Grupp, T. W. Ebbesen, and H. J. Lezec, Phys. Rev. B **58**, 6779 (1998).
[11] D. Maystre and M. Nevière, J. Opt. (Paris) **8**, 165 (1977).
[12] E. Popov, L. Tsonev, and D. Maystre, Appl. Opt. **33**, 5214 (1994).
[13] T. Lopez-Rios, D. Mendoza, F. J. Garcia-Vidal, J. Sanchez-Dehesa, and B. Pannetier, Phys. Rev. Lett. **81**, 665 (1998).
[14] Ph. Lalanne, J. P. Hugonin, S. Astilean, M. Palamaru, and K. D. Möller, J. Opt. A: Pure Appl. Opt. **2**, 48 (2000).
[15] D. Maystre and M. Nevière, J. Opt. (Paris) **9**, 301 (1978).
[16] P. Vincent, Opt. Commun. **26**, 293 (1978).
[17] G. H. Derrick, R. C. Mc Phedran, D. Maystre, and M. Nevière, Appl. Phys. **18**, 39 (1979).
[18] R. C. Mc Phedran, G. H. Derrick, M. Nevière, and D. Maystre, J. Opt. (Paris) **13**, 209 (1982).
[19] *Electromagnetic Theory of Gratings* edited by R. Petit (Springer-Verlag, Berlin, 1980).
[20] R. E. Collin, *Field Theory of Guided Waves*, 2nd ed. (IEEE, New York, 1991).
[21] L. Li, J. Opt. Soc. Am. A **14**, 2758 (1997).
[22] L. C. Botten, M. S. Craig, R. C. Mc Phedran, J. L. Adams, and J.

T. Andrewartha, Opt. Acta **28**, 413 (1981).
[23] L. C. Botten, M. S. Craig, and R. C. Mc Phedran, Opt. Acta **28**, 1103 (1981).
[24] G. Tayeb and R. Petit, Opt. Acta **31**, 1361 (1984).
[25] J. R. Andrewartha, J. R. Fox, and I. J. Wilson, Opt. Acta **26**, 69 (1979).
[26] J. R. Andrewartha, J. R. Fox, and I. J. Wilson, Opt. Acta **26**, 197 (1979).
[27] E. Popov and L. Tsonev, Surf. Sci. **271**, L378 (1992).
[28] A. Sentenac and D. Maystre, J. Mod. Opt. **45**, 785 (1998).
[29] H. Bremmer, Commun. Pure Appl. Math. **4**, 105 (1951).
[30] M. Born and E. Wolf, *Principles of Optics*, 6th ed. (Pergamon, Oxford, 1980).
[31] A. Wirgin and T. Lopez-Rios, Opt. Commun. **48**, 416 (1984); T. Lopez-Rios and A. Wirgin, Solid State Commun. **52**, 197 (1984).
[32] M. Nevière, E. Popov, R. Reinisch, and G. Vitrant, *Electromagnetic Resonances in Nonlinear Optics* (Gordon and Breach, Reading, MA, 2000).
[33] L. Li, J. Opt. Soc. Am. A **13**, 1024 (1996).
[34] F. Montiel, M. Nevière, and P. Peyrot, J. Mod. Opt. **45**, 2169 (1998).
[35] L. Li, J. Opt. Soc. Am. A **13**, 1870 (1996).
[36] Ph. Lalanne and G. M. Morris, J. Opt. Soc. Am. A **13**, 779 (1996).
[37] G. Granet and B. Guizal, J. Opt. Soc. Am. A **13**, 1019 (1996).